Particle identification below threshold with AMS-02 RICH detector *

Zi-Yuan Li[1,2;1)] C.Delgado[3)] F.Giovacchini[3)] J.Hoffman[4)] S.Haino[2)]

[1] School of Physics, Sun Yat-Sen University, Guangdong, 510275
[2] Institute of Physics, Academia Sinica, Taipei, 11529
[3] Centro de Investigaciones Energeticas, Mediambientales y Tecnologicas (CIEMAT), Madrid, E-28040
[4] Physics and Astronomy Department, University of Hawaii, Hawaii, 96822

arXiv:1611.02301v1 [physics.ins-det] 7 Nov 2016

Abstract: The Alpha Magnetic Spectrometer (AMS-02) was installed on the International Space Station (ISS) and it has been collecting data successfully since May 2011. The main goals of AMS-02 are the search for cosmic anti-matter, dark matter and the precise measurement of the relative abundance of elements and isotopes in galactic cosmic rays. In order to identify particle properties, AMS-02 includes several specialized sub-detectors. Among them, the AMS-02 Ring Imaging Cherenkov detector (RICH) is designed to provide a very precise measurement of the velocity and electric charge of particles. A method to reject the dominant electron background in antiproton identification using the AMS-02 RICH detector as a veto will be described. By using the collected cosmic-rays data, electron contamination can be well suppressed within 3% with $\beta \approx 1$, while keeping 76% efficiency for antiprotons below the threshold.

Key words: AMS-02, Cosmic ray antiproton, RICH detector, Aerogel Radiator, Cherenkov radiation, Particle identification

PACS: 29.40.Ka

1 Introduction

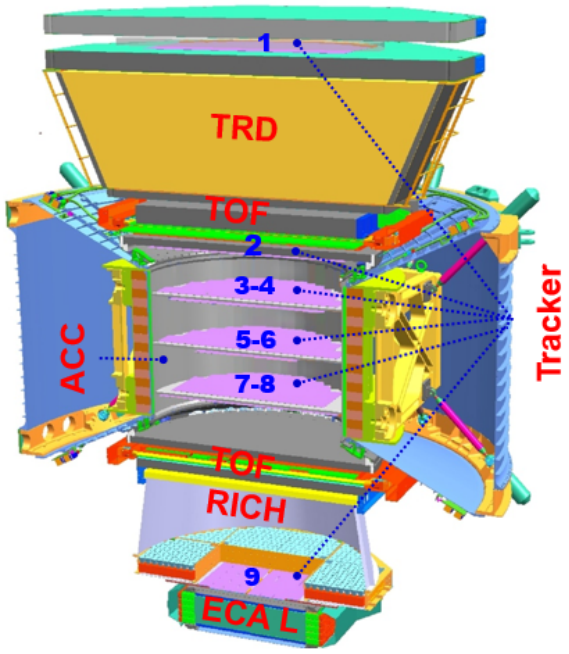

Fig. 1: Schmatic view of AMS-02 detector.

The AMS-02 detector is a general purpose, high energy physics detector described in detail in [1]. It is designed to measure cosmic ray particles in the energy range from 1 GV to a few TV. The detector consists of the following subsystems: a nine-layer silicon tracker[2], seven of which are surrounded by a permanent magnet[3]; a transition radiation detector (TRD)[4]; four planes of time of flight scintillator counters (TOF)[5]; an array of anticoincidence counters (ACC)[6]; a ring imaging Cherenkov detector (RICH)[7]; and an electromagnetic calorimeter (ECAL)[8].

The silicon tracker, together with the magnet provides precise measurement of particle rigidity (defined as R=p/Z, where p is particle momentum and Z its charge), its incoming direction and charge. The maximum detectable rigidity (MDR) over the 3 m lever arm from layer 1 (L1) to layer 9 (L9) is ∼2 TV for electrons, 2 TV for protons and 3.2 TV for helium. The TRD is designed to distinguish between hadrons and leptons with the use of transition radiation process. The four planes of TOF scintillator counters (two above and two below the magnet) provide fast trigger, particle velocity, incoming direction and charge. The 16 ACC counters form a cylindrical shell between the magnet and the tracker. Adjacent counters, combined, provide 8 readout sectors to reject cosmic rays entering the tracker from the side.

Received Day Month Year
∗ Supported by the China Scholarship Council (CSC) under Grant No.201306380027.
1) E-mail: ziyuan.li@cern.ch
©2016 Chinese Physical Society and the Institute of High Energy Physics of the Chinese Academy of Sciences and the Institute of Modern Physics of the Chinese Academy of Sciences and IOP Publishing Ltd

RICH detector measures particle velocity and charge. Combined with the tracker information, the RICH and the TOF allow for particle mass separation. The ECAL allows for separation between hadrons and leptons independently of the TRD. A detailed schematic view of AMS-02 detector is presented in Fig. 1.

2 Description of the RICH detector

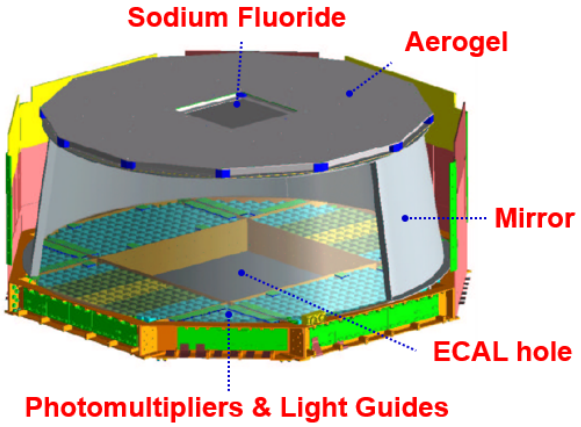

Fig. 2: Layout of AMS-02 RICH detector.

The RICH detector of AMS-02 is located between the Lower TOF and the ECAL. By providing precise measurements of velocity and absolute charge of incoming cosmic-rays, it plays a very important role in particle identification. As illustrated in Fig. 2, from top to the bottom, the RICH detector is composed of three main parts: a radiator plane where Cherenkov light is emitted, a high reflectivity mirror to increase detection efficiency, and a detection plane made of photomultiplier matrix and light guides[9–11]. The detection plane has a hole at the center to minimize the amount of material in front of the ECAL. A cone of Cherenkov light is emitted when an incoming charged particle crosses the radiator material with a velocity (β) greater than the Cherenkov threshold ($\beta_{thr} = \frac{1}{n}$) for this medium with reflective index (n). The aperture angle of the emitted photons with respect to the radiating particle direction is known as the Cherenkov angle (θ_c), which is connected to velocity according to equation Eq. 1 [12]:

$$\beta = \frac{1}{n \cdot cos(\theta_c)}. \quad (1)$$

In AMS-02, the RICH radiator plane includes two different radiators: 16 squared tiles of Sodium Fluoride (NaF) with dimensions $8.5 \times 8.5 \times 0.5$ cm^3 in the center covering $\sim 10\%$ of the RICH acceptance, and 92 silica aerogel tiles (AGL) with dimensions $11.5 \times 11.5 \times 2.5$ cm^3 surrounds the NaF radiator. The Cherenkov threshold for AGL is $\beta_{thr,AGL} \sim 0.95$, while for NaF, it is $\beta_{thr,NaF} \sim 0.75$. As compared to AGL, the NaF radiator allows to detect particles in a wider velocity range. Moreover, particles passing through NaF will generate Cherenkov radiation with larger Cherenkov angle, which increases the detector acceptance for particle trajectories pointing towards the ECAL.

In the following paper, we only discuss about AGL radiator due to the fact that the particle identification method below threshold is valid only for AGL radiator for rigidity range 1 - 3 GV.

3 Particle Identification Method

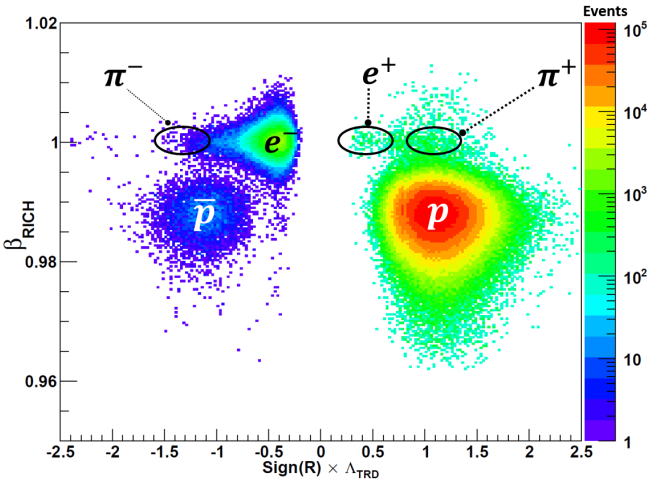

Fig. 3: Negative rigidity and positive rigidity data samples in the (β_{RICH} - Λ_{TRD}) plane for the absolute rigidity range 5.4 - 6.5 GV. The contributions of $\bar{p}$, p, e^+, e^-, π^+ and π^- are clearly seen. The antiproton signal is well separated from the backgrounds.

In AMS-02, particle identification is done by using measurement from different detectors[13]. At high energies ($|R| > 10$ GV) electrons and hadrons (such as antiprotons, pions, or kaons) can be identified in the TRD with the TRD estimator Λ_{TRD}[14] and also in ECAL with the ECAL estimator based on a boosted decision tree algorithm, which is constructed from the shower shape in the ECAL[15–17]. In AMS-02 the RICH velocity resolution for charge 1 particles has been measured using in-flight calibrated data to be $\Delta\beta/\beta \sim 10^{-3}$ in the case of AGL radiator[18]. Therefore at middle energies ($|R|$ between 3 to 10 GV), velocity measured with the RICH detector β_{RICH} together with the Λ_{TRD} is used to separate the antiproton signal from light particles (e^- and π^-, K) background. ECAL is not used for particles passing through AGL. As an illustration on Fig. 3, antiproton signal and background are well separated in the (β_{RICH} - Λ_{TRD}) plane for the absolute rigidity range 5.4 - 6.5 GV using collected cosmic rays data. For $\bar{p}$ below the threshold ($|R| < 3$ GV), this paper provides an innovative approach to use AMS-02 RICH detector as a threshold-type aerogel Cherenkov detector to reject the remaining electron backgound in the identification of cosmic ray antiproton after Λ_{TRD} selection.

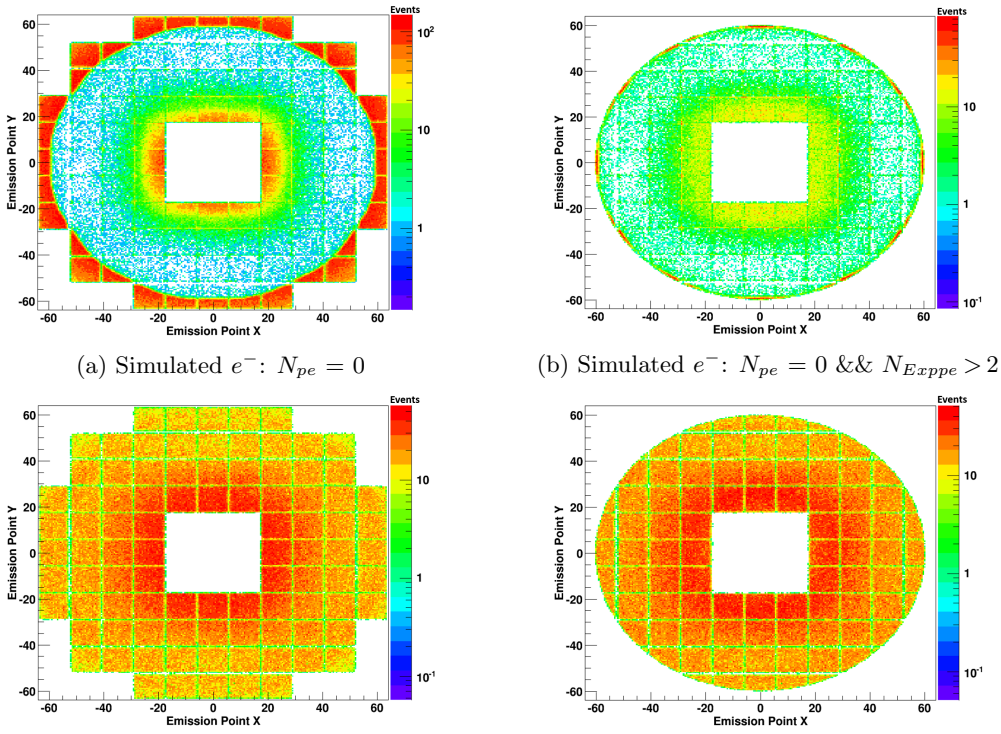

(a) Simulated e^-: $N_{pe}=0$

(b) Simulated e^-: $N_{pe}=0$ && $N_{Exppe}>2$

(c) Simulated p: $N_{pe}=0$

(d) Simulated p: $N_{pe}=0$ && $N_{Exppe}>2$

Fig. 4: Particle emission coordinates in Aerogel in the X-Y plane of the detector.

3.1 Basic Idea

The corresponding rigidity for p ($\bar{p}$) with $\beta=\beta_{thr,AGL}$ is ~ 3 GV. Therefore below ~ 3 GV, p will not produce Cherenkov light when passing through AGL, while for electrons (for which $\beta\approx 1$ in this rigidity range) Cherenkov light emission is expected. Based on this concept, we require that the number of photoelectrons[9] (N_{pe}) detected by RICH equals to zero in order to reject electrons. The N_{pe} signal produced by the charged particle in the impact point of the detection plane due to energy losses in light guide have already been subtracted.

However, in order to further reject electrons, additional effects should be considered. Events with zero photoelectrons could be electrons where Cherenkov radiation was lost or absorbed due to one of possible effects like Rayleigh Scattering, total reflection in aerogel radiator, reflection or absorption on the mirror surface, falling into non-active area, light guide losses, and the like.

To see the evidence of those effects, Monte-Carlo samples of electrons and protons in rigidity range 1 to 3 GV were produced in GEANT 4.10.1 package[19, 20]. The samples underwent the same process of reconstruction method as cosmic ray data. From the emission coordinates of incoming particle in aerogle radiator, we can see the difference between e^- and p. As shown in Fig. 4a, the majority of e^- events after requirement of $N_{pe}=0$ tend to distribute around the region outside of the top mirror radius and near the ECAL hole region. For p events (Fig. 4c), the distribution is basically uniform except the center region due to larger acceptance.

In order to remove as much of the electron background as possible while keeping high proton efficiency, a Toy Mont Carlo Simulation method is used to calculate the number of expected photoelectrons (N_{Exppe}) which takes into account all those radiation losses and absorption.

3.2 Toy Mont Carlo Simulation

For each Toy Monte-Carlo Simulation event, assuming it is an electron, combined with rigidity from tracker we can generate a homogeneous cone of photons with Cherenkov angle $\theta_c=\arccos(\sqrt{R^2+m_e^2}/nR)$ (m_e is the mass of electron). Then we can use a ray tracing integration method to compute the detection efficiency after taking into account all losses and absorption. To get the number of expected photoelectrons N_{Exppe}, we need to multiply the detection efficiency by the expected light yield, which at $\beta=1$ is proportional to $(n^2-1)/n^2$ and depends linearly on the sample's thickness and radiator absorption.

We require $N_{Exppe}>2$ to select particles that pass through good geometry region and are good enough to reconstruct a ring for electron events. The cut effect can be clearly seen in Fig. 4b and Fig. 4d. For simulated e^-, the cut efficiency is $\sim 20\%$ while for p, the efficiency is

$\sim 88\%$.

4 Data selection

Five years data have been analysed starting from May of 2011 to May of 2016. During this period, over 80 billion cosmic-rays events have been recorded. Events considered in this analysis were collected during normal detector operation, i.e. during time periods when the AMS Z-axis is pointing within 40° of the local zenith and when the ISS is not in the South Atlantic Anomaly.

Further selection requires a track in the inner tracker, matching a track inside the TRD. The velocity in the TOF is required to be $\beta_{TOF} > 0.3$, corresponding to a downward-going particle. Moreover, the dE/dx measurements in the TRD, the TOF, and the inner tracker must be consistent with $|Z| = 1$. The accuracy of track reconstruction, the $\chi^2/d.f.$ is required to be less than 10 both in the bending and non-bending projections in order to maximize the accuracy of the track reconstruction. The track, extrapolated from the Tracker outwards should pass through both surfaces (upper and lower) of the aerogel. Good geometry region is chosen with requirement of $N_{Exppe} > 2$. The events in focus are those with rigidity below aerogel threshold for protons ($|R| < 3$ GV).

Events satisfying the selection criteria are classified into two categories - positive and negative rigidity events. In positive rigidity population, 99.9% are pure protons with almost no background. Among negative rigidity events there are antiprotons and several background sources : electrons, light negative mesons (π^- and negligible amount of K^-), produced in the interactions of primary cosmic rays with the detector material.

To evaluate the performance of this particle identification method, TRD estimator Λ_{TRD} is used as an independent detector to select pure proton and pure electron sample.

5 Performance

The Normalized N_{pe} distribution of cosmic ray protons (in blue) and electrons (in red) in the rigidity range $1.16-1.51$GV is shown in Fig. 5. As it can be seen from the plot, majority of protons concentrate at 0 while for electrons the distribution is wider. From a detailed analysis, the upper tail of the histogram produced by below-threshold particles can be attributed to several different sources as δ-rays, accidental particle crossing the radiator, scintillation light produced in the radiator, and the like. The peak at zero for electrons is due mainly to events that cannot be reconstructed due to a statistical fluctuation of the real number of photoelectrons in the event.

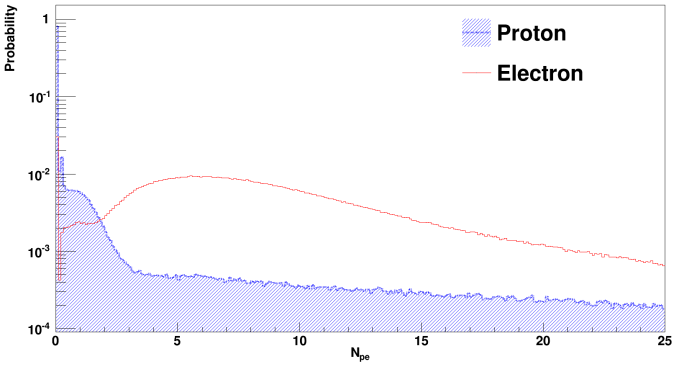

Fig. 5: Normalized N_{pe} distribution for cosmic ray protons (in blue) and electrons (in red) in rigidity range $1.16-1.51$GV.

To study the performance of this particle identification method, we can make a tight cut by applying $N_{pe} = 0$ and see how the protons (in blue) and electrons (in red) cut efficiency changes with rigidity, as shown in Fig. 6. Here the inverted filled triangle points are cosmic ray data while regular empty triangle points are simulated data. The simulated data reproduce well the result from cosmic ray data. For protons, the cut efficiency is about 76% and keeps almost constant up to 3GV. For electrons, the cut efficiency is about 3%.

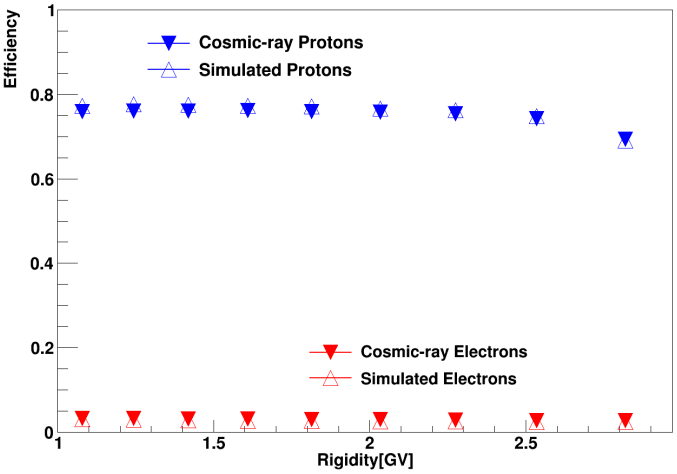

Fig. 6: $N_{pe} = 0$ cut efficiency changes with rigidity. Inverted filled triangle points are cosmic ray protons (in blue) and electrons (in red) while regular empty triangle points are simulated data.

After applying $N_{pe} = 0$ cut on cosmic ray data, velocity measured with the TOF detector β_{TOF} together with the Λ_{TRD} is used to separate the antiproton signal from light particles background. As shown in Fig. 7, a well enhanced $\bar{p}$ signal in the (β_{TOF} - Λ_{TRD}) plane for the absolute rigidity range 1.16 - 1.51 GV can be seen.

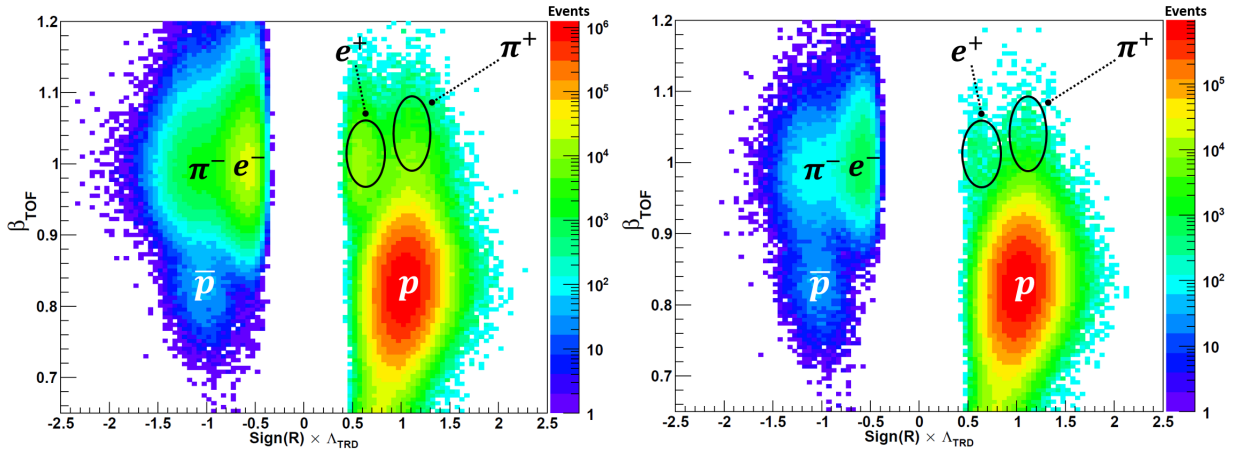

(a) Before applying $N_{pe} = 0$ cut

(b) After applying $N_{pe} = 0$ cut

Fig. 7: Negative rigidity and positive rigidity data samples in the (β_{TOF} - Λ_{TRD}) plane for the absolute rigidity range $1.16-1.51$GV. The contributions of $\bar{p}$, p, e^+, e^-, π^+ and π^- are clearly seen. After applying $N_{pe} = 0$ cut, the antiproton signal is better enhanced from the backgrounds.

6 Conclusions

A dedicated method to use AMS-02 RICH detector as threshold-type aerogel Cherenkov detector has been discussed. The cut efficiency of this method derived from cosmic ray can be well reproduced by the simulated data. Electron contamination can be well suppressed within 3% with $\beta \approx 1$, while keeping 76% efficiency for protons below the threshold.

With this method, antiproton signal can be enhanced in a better way from background events of electrons and light negative mesons in the (β_{TOF} - Λ_{TRD}) plane.

References

1 A.Kounine, International Journal of Modern Physics E, **21**: 123005 (2012)
2 B.Alpat et al, Nucl. Instrum. Methods A, **613**: 207 (2010)
3 K.Luebelsmeyer et al, Nucl. Instrum. Methods A, **654**: 639 (2011);
4 Th.Kirn, Nucl. Instrum. Methods A, **706C**: 43 (2013); Ph.Doetinchem et al, Nucl. Instrum. Methods A, **558**: 526 (2006); F.Hauler et al, IEEE Trans. Nucl. Sci, **51**: 1365 (2004)
5 A.Basili et al, Nucl. Instrum. Methods A, **707**: 99 (2013); V.Bindi et al, Nucl. Instrum. Methods A, **623**: 968 (2010)
6 Ph.Doetinchem et al, Nucl. Phys. B, **197**: 15 (2009)
7 P.Aguayo et al, Nucl. Instrum. Methods A, **560**: 291 (2006); B.Baret et al, Nucl. Instrum. Methods A, **525**: 126 (2004); J.Casaus, Nucl. Phys. B (Proc. Suppl.), **113**: 147 (2002)
8 C.Adloff et al, Nucl. Instrum. Methods A, **714**: 147 (2013)
9 M.Aguilar-Benitez et al, Nuclear Instruments and Methods in Physics Research Section A, **614**: 237 249 (2010)
10 L.Arruda, F.Barao, P.Goncalves, and R.Pereira, Nuclear Physics B Proceedings Supplements, **172**: 32 35 (2007)
11 D.Casadei, Nuclear Physics B Proceedings Supplements, **125**: 303 307 (2003)
12 J.Seguinot and T.Ypsilantis, Nucl. Instr. and Meth. A, **343**: 1 (1994)
13 M.Aguilar et al, AMS Collaboration, Phys. Rev. Lett. **117**: 091103 (2016)
14 Z.Weng, Particle Identification Using Transition Radiation Detector and Precision Measurement of Cosmic Ray Positron Fraction with the AMS-02 Experiment, Ph.D Thesis(Guangdong: School of Physics, Sun Yat-Sen University, 2013)
15 F.Cadoux et al, Nuclear Physics B Proceedings Supplements, **113**: 159 165 (2002)
16 Z.Li et al, Chinese Physics C, **37**(02): 026201 (2013)
17 Z.Li et al, Chinese Physics C, **38**(05): 056203 (2014)
18 F.Giovacchini, et al, AMS Collaboration, Nuclear Instruments and Methods in Physics Research Section A, **766**: 57 - 60 (2014)
19 S.Agostinelli, et al, Nuclear Instruments and Methods in Physics Research Section A, **506**: 250 (2003)
20 J.Allison, et al, IEEE Trans. Nucl. Sci, **53**: 270 (2006)